PILOT TEST FOR CONTINUOUS PRODUCTION OPTIMIZATION USING A DIGITAL SOLUTION ON PERMIAN BASIN WELLS

Daniel Croce, Hardik Zalavadia, Haiwen Zhu, Arsalan Adil, Timothy Credeur
Xecta Digital Labs

Timothy Credeur and Kevin McNeilly, BPX

ABSTRACT

Objective/Scope

Optimizing production across unconventional assets requires rapid identification of well performance anomalies, efficient artificial lift optimization, and scalable evaluation of intervention opportunities such as acid jobs and lift-system transitions. Traditional surveillance workflows struggle to keep pace with high well counts, changing lift designs, and evolving reservoir conditions. This pilot study focused on a digital production optimization system deployed on 441 wells equipped with gas lift and ESPs in the Permian Basin. The scope included daily surveillance for production optimization, evaluation of artificial-lift transition scenarios, defining surface injection-pressure management criteria for multi-well gas-lift systems, and systematically assessing acid-job performance to determine optimal implementation conditions.

Methodology

A web-based production optimization platform, integrating comprehensive physics-based modeling with advanced AI-driven analytics, was used to continuously process historical and daily production data. The system employs a novel transient reservoir pressure estimation based on dynamic drainage volume computation with multiphase well modeling to characterize reservoir inflow performance, artificial-lift behavior, and deviations from design operating envelopes. Daily computations include productivity-index forecasting, bottomhole pressure tracking, and opportunity identification for lift adjustments (e.g., gas-lift injection tuning, ESP frequency optimization). Statistical analysis of historical acid-job interventions was conducted to correlate treatment success with inflow performance constraints identified and the chemical composition of produced fluids, particularly indicators of solids-related deposition risk. Multi-well gas lift modeling was used to evaluate injection-pressure requirements across groups of wells sharing same compressors

Case Study Results and Observations

Implementation of the platform's daily optimization recommendations yielded a measurable and repeatable impact across the 441-well asset. Wells for which recommendations were adopted delivered an average of 6% incremental oil production, primarily driven by optimized gas-lift injection rates and ESP operating frequencies. Concurrently, the field achieved over a 20% reduction in average gas-lift usage, reflecting more efficient allocation of lift gas. The acid-job evaluation workflow identified the most favorable PI opportunities by tracking PI trends associated with inflow issues and treatment success, providing operators with predictive criteria to avoid treatments likely to result in insufficient inflow improvement. Multi-well gas-lift network analysis produced clear guidelines for managing surface injection-pressure constraints, optimizing the allocation of gas for production improvement among wells sharing the compressor.

Novelty and Significance

This work demonstrates how an integrated hybrid modeling system—combining physics-based flow dynamics with data-driven techniques—can transform daily surveillance and optimization workflows for unconventional asset management. Unlike traditional manual review processes, the platform delivers continuous, scalable, and objective recommendations for lift-control adjustments and conversions, well interventions, and facility-level gas-lift management. The structured analysis of acid-job performance provides a reliable framework for diagnosing treatment potential from both reservoir-productivity and fluid-chemistry perspectives, minimizing ineffective interventions. The simultaneous optimization of ESPs, gas lift, and multi-well injection-pressure management highlights the system's ability to coordinate decisions across diverse lift systems and facility bottlenecks. The pilot results confirm the value of deploying automated, physics-informed digital solutions that enhance operational efficiency, reduce resource consumption, and support proactive, field-wide production management.

1. INTRODUCTION

441 wells in the Permian Basin equipped with gas lift systems and electrical submersible pumps were monitored using a digital supervision system. The system delivered daily recommendations for set point optimization of the artificial lift systems in place, as well as evaluation of artificial-lift transition scenarios, and the analysis of acid job performance for determination of expected impact on the production of the wells and determination of the right moment and conditions for implementation.

The digital monitoring system used integrates a comprehensive physics-based model with AI-driven analytics, to continuously process production data, providing a perspective connected from the first to the latest day of production. The solution is web based, connecting to the daily production and wellhead data for each well, allowing the execution of daily and instantaneous calculation, while reducing the required time for update and maintenance.

2. METHODOLOGY

2.1. Transient Well performance (TWP)

The system employs a novel transient reservoir pressure estimation based on dynamic drainage volume computation, including multiphase well models to characterize reservoir inflow performance, artificial-lift behavior, and deviations from design operating envelopes.

Figure 1 – Transient well performance modeling scheme (Parekh, Zalavadia et al. 2025)

The core principle of TWP is that the drainage volume of the hydrocarbon reservoir expands over time, albeit with an undefined geometry. By leveraging the diffusive time-of-flight method, the drainage volume is estimated while ensuring a no-flow outer boundary, with reservoir withdrawals accounted for via cumulative production data. Under the SPSS assumption, high-resolution material balance calculations (e.g., on a daily basis) provide a dynamic assessment of reservoir pressure depletion and average reservoir pressure trends within the contacted drainage volume at any given time.

2.2. Applications of TWP

TWP leverages routinely available production data, combined with pressure-volume-temperature (PVT) properties and flowing bottomhole pressure measurements (Molinari et al. 2019a). The framework accommodates variable production rates, pressure depletion, nonlinear pressure-dependent PVT properties, and multiphase flow conditions

across diverse artificial lift methods, including natural flow, gas lift, electrical submersible pumps (ESP), and sucker rod pumps. The insights derived from TWP enable field-scale automation for critical production engineering applications such as inflow/outflow opportunity identification, anomaly detection, PI-based forecasting, artificial lift optimization, and production scenario modeling.

2.3. Drainage Volume Estimation

In the absence of a detailed well and reservoir model, Dynamic Drainage Volume (DDV) is estimated using pressure and rate data as shown on equation 1 (Xue et al. 2018, Molinari et al. 2019b):

$$V_d \approx \frac{1}{c_t \frac{d}{dt_e}(RNP)} \qquad \text{Eq. 1}$$

This formulation represents the effective contacted pore volume at any given time step, tracking the extent of pressure propagation within the reservoir. Like the concept of the radius of investigation in homogeneous formations, it delineates the diffusive time-of-flight contours within an irregularly shaped drainage area, encompassing both the stimulated and unstimulated reservoir matrix. The RNP-based calculation offers a representative model of production behavior under a standardized reference rate.

2.3.1. Material Balance with an Expanding Control Volume

Traditional material balance methods are strictly applicable in steady-state or pseudo-steady-state conditions, where reservoir boundaries have been fully contacted. However, unconventional reservoirs seldom reach boundary-dominated flow due to their low permeability, where even after fracture connectivity is established, additional matrix volume continues to contribute to flow over time.

To address this, an expanding control volume approach is implemented. This method conceptualizes reservoir drainage as an evolving boundary, analogous to an expanding balloon, where pressure contours define the outer boundary's progression. The SPSS framework approximates transient flow as a sequence of pseudo-steady-state snapshots, with drainage volume computed at each time step as shown in Figure 2. Given that the system is defined by a no-flow (DDV concept), outer boundary at each instant, energy loss due to production can be directly estimated, allowing for accurate reservoir depletion calculations. The use of daily production increments enhances the precision of material balance assessments.

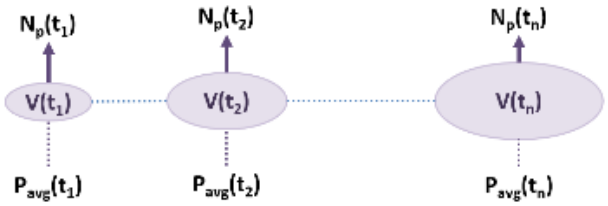

Figure 2. Material Balance applied to succession of pseudo-steady-state conditions with expanding drainage volume (Bimal, Zalavadia et al. 2025)

For liquid systems, the general material balance equation accounts for the expansion of liberated gas, the expansion of liquids, the change in the pore volume and the remaining liquids and the underground withdrawal. Considering these principles, this equation can be adapted to unconventional reservoirs with no gas cap or active aquifer.

2.4. Transient Productivity Index

As outlined by Molinari et al. (2019a, 2019b), the productivity index (PI) serves as a robust diagnostic metric, reflecting true reservoir inflow potential by normalizing production volumes with flowing pressure data. PI incorporates depletion effects and pressure-volume-temperature (PVT) properties, making it a superior alternative to rate-time-based decline curve analysis (DCA) and type curves, which often introduce biases due to variable operating conditions.

In unconventional reservoirs, PI is inherently transient and must be updated dynamically at each time step. By linking production rates with pressure drawdown behavior, PI provides a quantitative basis for optimizing well performance under different operational strategies, including artificial lift adjustments and reservoir management decisions. Daily computations of the productivity-index, allow the statistical analysis of historical acid-job interventions to correlate treatment success with inflow performance constraints,

$$q_l(t) = PI(t) * \left(p_{avg}(t) - p_{wf}(t)\right) \qquad \text{Eq. 2}$$

2.4.1. Bottomhole Pressure (BHP)

The TWP approach highlighted above requires accurate daily estimates of bottomhole pressure (BHP), making well outflow modeling essential for production scenario analysis and artificial lift (AL) optimization. The downhole flowing pressure at the reservoir inflow depth is critical for assessing well performance. However, in unconventional wells, continuous BHP measurement data is rarely available, while wellhead pressure (WHP) is typically measured in every well. As mentioned by Wortmann (Wortmann, Zalavadia et. Al, 2025) “(…) permanent downhole gauges are uncommon and, when available, are

often memory-based or limited to monitoring ESP intake pressure for short durations (…)". Consequently, BHP must be computed from using the surface pressure and rate data. The estimation of the BHP can be approached using steady-state multiphase flow correlations to model the pressure profile along the wellbore, accounting for the static, frictional, and acceleration related losses, as well as the pressure contribution from artificial lift systems (e.g., ESP, rod pump) as shown in equation 3. In gas-lifted wells, the effect of gas injection in reducing liquid column density is also incorporated:

$$\Delta P = \Delta P_{static} + \Delta P_{friction} + \Delta P_{acceleration} - \Delta P_{lift} \quad \text{Eq. 3}$$

The multiphase flow model considers PVT data, wellbore geometry and production parameters. To maintain accuracy, the model must be updated continuously to reflect modifications in wellbore configuration and artificial lift installations, such as tubing replacements or new lift mechanisms. BHP calculations are performed at the same resolution as rate data, whether from metering, allocation, or well tests. This process has been automated at the field scale, enabling real-time BHP computation as part of digital production surveillance workflows (Molinari et al. 2019a).

While multiphase flow correlations provide reasonable estimates, they may not always capture pressure gradients accurately under varying operational conditions. In such cases, hybrid physics- and data-driven modeling approaches can improve accuracy, as detailed in Molinari and Sankaran (2021). The primary objective remains to generate a reliable, continuous BHP estimate for improved characterization of dynamic production behavior.

2.4.2. Gas lift BHP

Bottomhole pressure in gas-lifted wells is calculated using multiphase flow correlations, considering counterflow gas from the wellhead toward the injection point and accounting for pressure changes due to temperature effects. The calculation considers the system configuration (multiple valves and an orifice, or slick tubing) and the production path (tubing or casing) to determine the injection point into the upward-flowing stream, as shown in Figure 3. Where the injection-pressure traverse exceeds that of the production stream, the model determines the injection depth, whether at a gas lift valve or the end of the tubing.

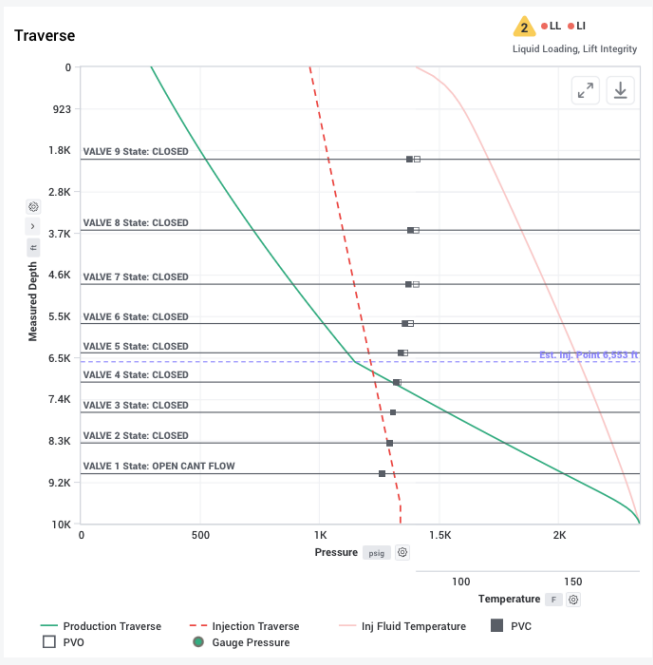

Figure 3 – Gas lift traverse diagram

If the pressure also exceeds the opening pressure of the gas lift valve, then the valve port depth is determined to be the point of injection. The amount of gas that can flow through the valve is computed, and the remaining gas flow rate is used to continue toward the next gas lift valve or the end of the tubing. When this point of injection falls between the depths of two gas lift valves, or before the end of slick tubing, it is interpreted as a “hole in tubing,” and “lift integrity” is flagged in the platform; this is confirmed using the production pressure gradient built from wellhead pressure.

2.4.3. ESP BHP

OPR (outflow performance relationship) or VLP (vertical lift performance) of ESP wells is obtained by traversing the pressure from the wellhead to the discharge of the ESP, and then computing the pump head to obtain the pump intake pressure (PIP). When comparing the computed PIP against the intake sensor of the ESP, head degradation and gas separation efficiency can be calculated to better understand pump performance. Additional considerations must be made to this process, as shown in Figure 4, when the pressure intake sensor fails:

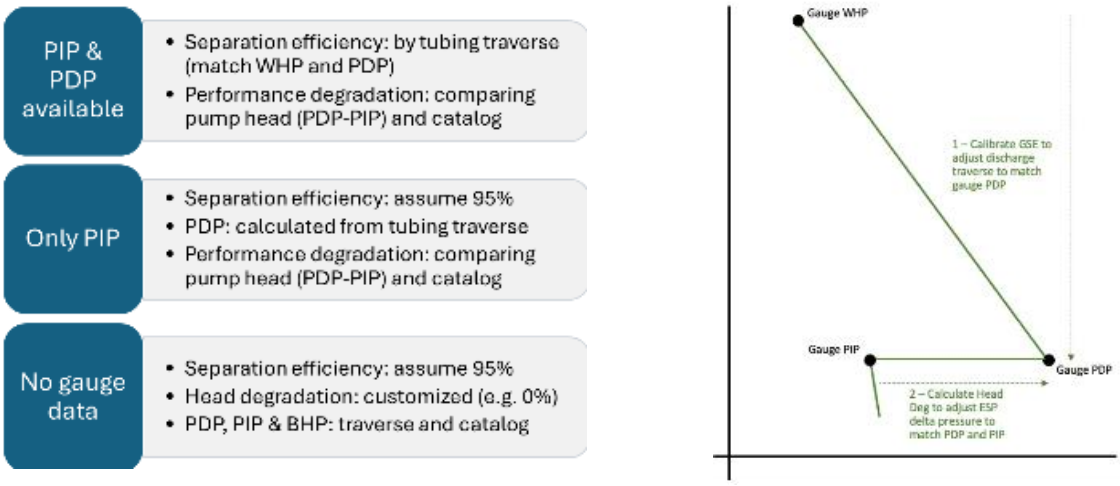

(a) (b)

Figure 4 - ESP traverse with WHP, PIP, and PDP. (a) Different scenarios (available gauge readings), (b) ESP well tubing pressure traverse logic (Wortmann, Zalavadia et al. 2025)

2.4.3.1 ESP Performance modeling

Determining the pressure traverse in the tubing of oil and gas wells requires analyzing how pressure varies along the wellbore, which is essential for both optimizing production and maintaining safe operations. In ESP wells equipped with a downhole gas separator, a key challenge is estimating its separation efficiency and the tubing gas rate from the measured total gas rate. This process involves multiple considerations: recording both surface and downhole data, evaluating fluid properties through a PVT model, calculating tubing pressure traverse with a pipe flow model, and assessing artificial lift performance via ESP behavior.

This study applies a widely used black oil model along with a pipe flow model to calculate the tubing pressure traverse. The black oil model simplifies phase behavior modeling by representing reservoir fluids as three phases: gas, oil, and water. After determining the downhole fluid properties, a multiphase pipe flow model is employed to estimate pressure losses caused by friction, elevation changes, and fluid acceleration in the tubing.

The surface rates used in this work come from regular well production allocation and well tests. The rates considered for the calculation of the pressure traverse differentiate between injected and reservoir sourced gas rates. Tubing traverse uses measured PIP and PDP directly if both gauge data are available. The gas rate in the tubing (Q_{g_tub}) is iteratively calculated until the calculated PDP from well head pressure (P_{wh}) matches the PDP computed from the tubing pressure traverse calculations. With that, the Q_{g_tub} and Q_{g_total} (total gas rate) are converted to the equivalent rates at the intake pressure

conditions, allowing to calculate a separation efficiency. Finally, performance degradation is calculated by comparing the downhole rates and head with the curves from the manufacturer (from a bench test). The processes followed for the tubing traverse and downhole separation efficiency calculation are summarized in Figure 5.

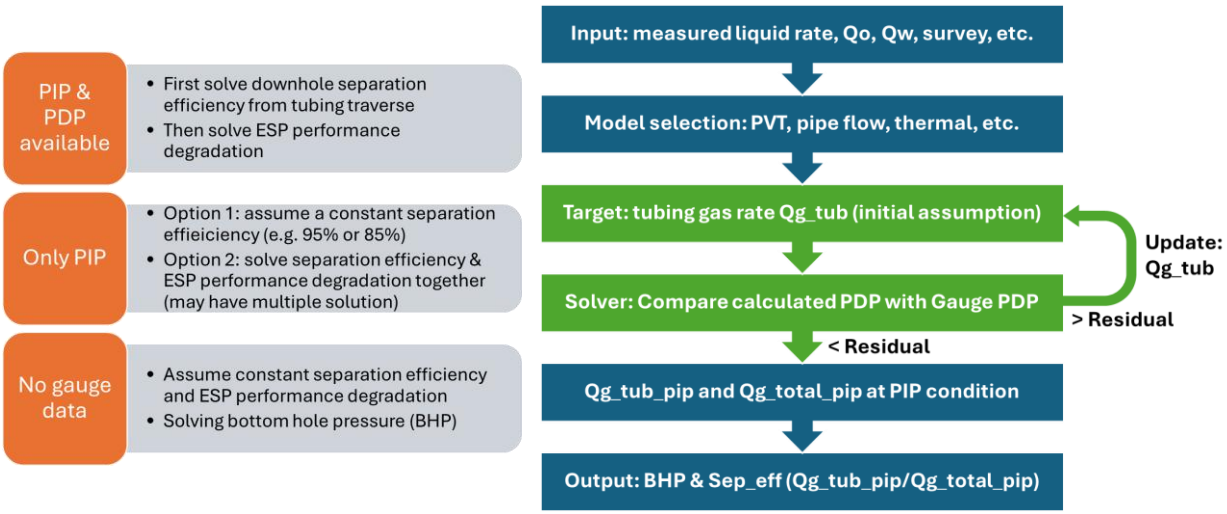

(a) Solution scenario (b) Tubing traverse solving procedure

Figure 5 Tubing traverse and downhole separation efficiency solving strategy (Wortmann, Zalavadia et al. 2025)

2.4.4. Multiphase flow modeling of an ESP stage

Evaluating the performance of an Electrical Submersible Pump (ESP) handling multiphase flow, requires a comprehensive consideration of the relation between the operating parameters and the interaction of the phases flowing within the stages of the pump. The most simple approach is to rely on affinity laws and homogeneous density of the mixture, which neglects effect of surging and possible gas locking as the gas volume fraction changes with the behavior of the reservoir and the increase of pressure along the stages of the equipment.

2.4.5. Gas volume fraction impact

Gas effects on pump performance pose a major challenge in ESP wells. There is no universal solution applicable to all ESPs. Empirical models and pump tests are typically limited to specific pump designs, while mechanistic models require detailed pump geometries, which are often unavailable to operating companies. The widespread use of gas-handling pumps further complicates the analysis, as these pumps break gas bubbles

into fine gas-water emulsions, potentially enhancing ESP performance rather than degrading it. This complexity explains why downhole ESP systems often integrate multiple components, including downhole separators, gas handler stages, mixed-type stages, and radial-type stages. This study adapts the mechanistic model from TUALP (Zhu et. al., 2022) and introduces simplified assumptions on ESP geometries. The main geometric parameters of the impeller such the radius and channel heights, are considered along with the slip gas void fraction, drag coefficients and size of the bubbles as well as some other coefficients, to reflect the impact that an increasing GVF has on the head at a certain rotating frequency, as shown on Figure 6, it can be observed the detriment on the head that a stage manifests at low rates when in the presence of gas, as pockets create along the inter-blade channel, limiting the flow of liquid out of the impeller, as well as how this impact increases when the GVF increases.

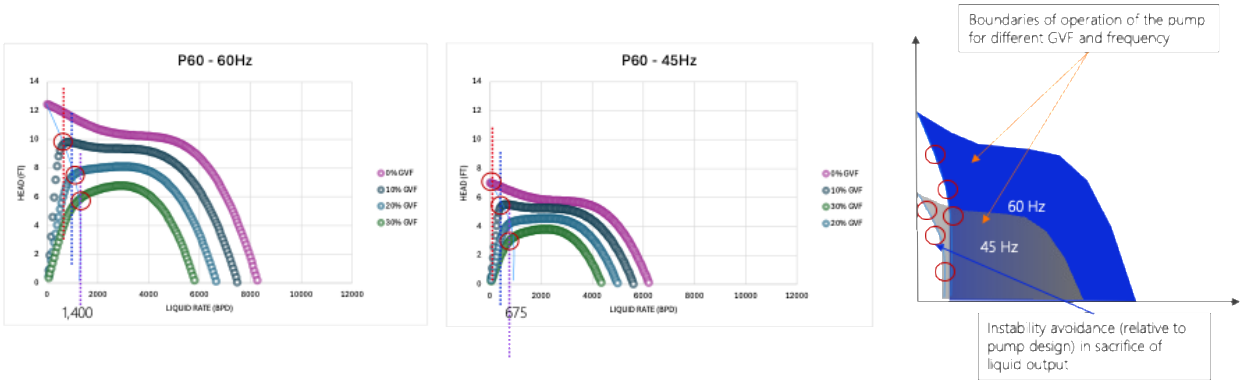

Figure 6 – Multiphase flow model effects on the head of an ESP stage.

When combined with affinity laws, the model allows to determine a more stable area of operation when the pump behavior becomes unstable due to the presence of gas. This way, the operation of the pump can be taken to a more stable zone, where gas interference and subsequent surging and gas locking are avoided.

2.4.6. Stage-by-stage performance and degradation calculation

The ESP stage-by-stage calculation procedure determines the pressure distribution across each pump stage by sequentially evaluating intake conditions, fluid properties, and downhole flow dynamics, which provides a better way of evaluating pump performance degradation. The process begins with the intake pressure per stage, influenced by downhole condition and gas-liquid separation efficiency. Next, fluid properties and downhole flow rate are assessed, and gas effect is introduced in next section. Finally, the outlet pressure per stage is calculated based on the intake pressure and ESP performance curves (head vs. flow rate), with the pressure increment at each stage added to determine the overall pump head. This iterative process shown in Figure 7 continues stage by stage until reaching the final outlet pressure, allowing engineers to optimize ESP design, evaluate performance degradation, and enhance artificial lift efficiency. In addition, it also considers different types of stages used in an ESP, e.g. gas

handler, mixed type, and radial type stages. The proposed method can also be used to calculate BHP in case gauge data is missing by assuming constant separation efficiency and pump performance degradation and then solving iteratively.

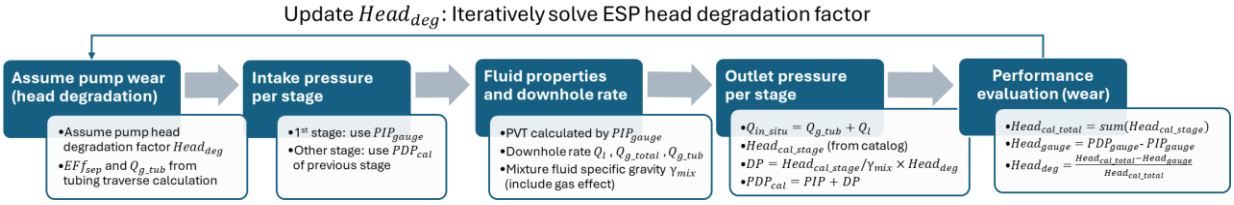

Figure 7 - ESP pump performance stage by stage calculation workflow

2.4.7. ESP tornado chart

Conventional pump charts fail to provide a clear perspective of an ESP arrangement when managing multiphase fluid flow. On a pump tornado chart, as provided in the employed surveillance tool, it is combined the ESP pump curves with the before mentioned stage-by-stage calibration and the in-situ flow rates and fluid properties. The gas handler effect on the total pump arrangement is also included on the chart, which can be observed at the right of the curve, as the flow rate capacity increases on a relatively low head area. Daily production measurements, are plotted in a color scale according to the frequency or date. Points that tend to move to the left with date (more red points are noted to the red than to the right pf the plot) indicate an increasingly unstable pump, that manages relatively lesser downhole flow rate, compared to its design BEP flow rate, as a result of the reservoir decline and the increase on gas volume fraction.

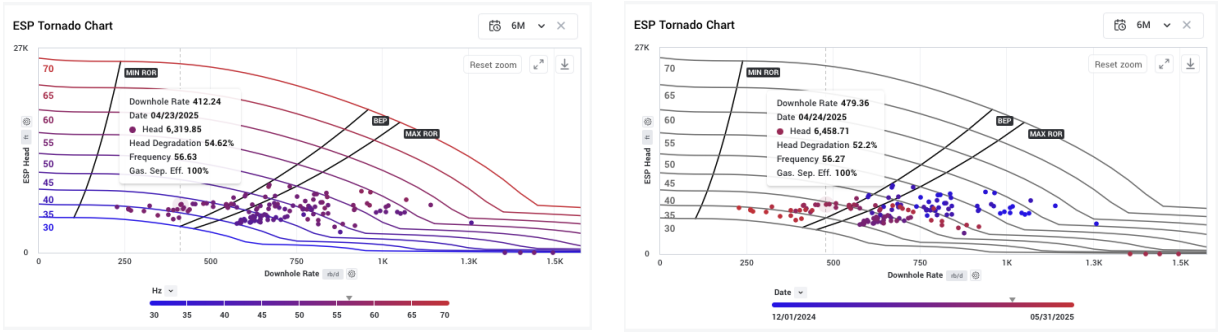

(a) Frequency based (b) Date based

Figure 8 - ESP Tornado chart

2.4.8. PID mode Amperage set point recommendation

The multiphase nature of the hydrocarbon reservoirs results in unstable operation of the ESPs as the gas volume fraction (GVF) increases with the life of the well. This represents

a challenge that requires special considerations for frequent adjustments of the operating setpoint of the pump. Uneven distribution of the gas phase along the inter-blade channels within an ESP stage, as well as a constantly variating fraction during the day, generate surging and even gas blocking effects within the pump. This causes sudden swings on the electric current demanded by the motor of the pump, that depending on the flowrate capacity of the stage arrangement, the volumetric rate of the fluids and the GVF, might exceed the operating limits defined by the manufacturer. This results in frequent shutdowns and extended downtimes.

To manage such pump swings, a “lookback algorithm” triggered by the magnitude of the electric current swings and the allowed maximum electric current of either the VSD or the pump motor, provided a recommendation to switch from “frequency mode” to “PID mode” with the corresponding electric current set point. As shown in Figure 9, the algorithm analyzed the electric current (in this case of the VSD) and corresponding frequency of the previous 7 days of operation of the equipment, and disregarding downtimes of the pump, it provided a statistically based electric current set point in which the amp swings were expected to be within smaller fluctuations, and remain below the maximum allowed operating electric current of the pump.

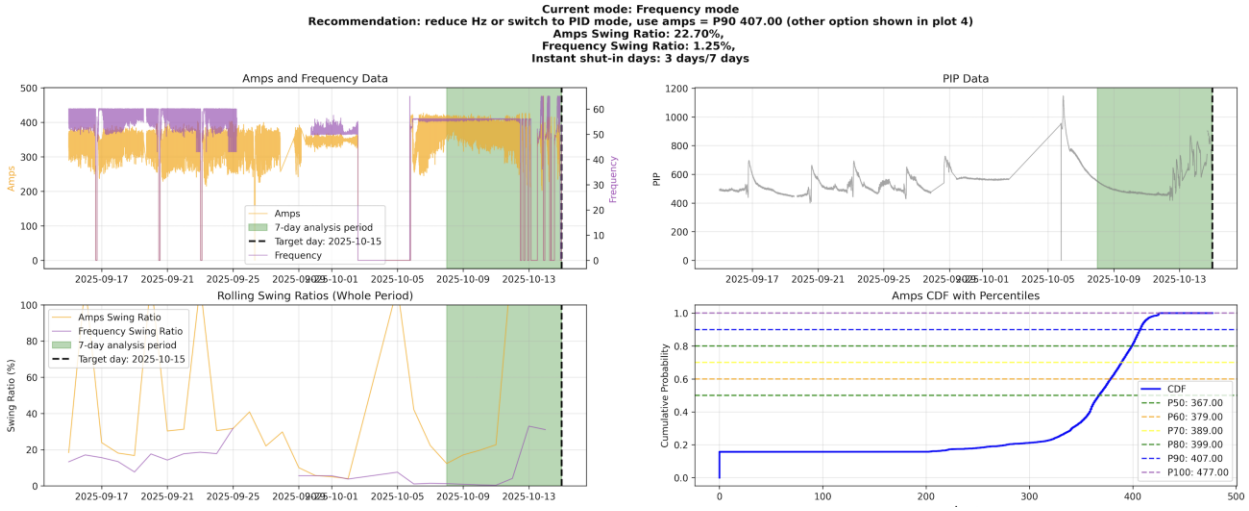

Figure 9- Considered variables for “PID” mode algorithm

Daily recommendations were provided to the engineers in the pilot test for adjustments in cases where the pump set point could not be increased but only adjusted for better flow rate management and extension of the ESP operating life. Whenever an ESP was lacking the PIP sensor data, this algorithm was implemented regardless of the swings on the electric current.

2.5. ESP setpoint optimization

Continuous estimation of setpoint opportunities is necessary to maximize cashflow from pump operations and improving the run life of the pump based on existing ESP

performance. Thus, dynamic estimation of pump head degradation and gas separation efficiency highlighted above becomes essential. The setpoint recommendation also needs to consider the prevailing reservoir and fluid conditions to allow for performing nodal analysis at different ESP frequencies. In unconventional reservoirs, modeling the fluid flow mechanism and hence estimation of reservoir pressures and PI is extremely challenging due to long transient flow, to dynamically track and thus scale across all the wells on a daily basis. In order to address this issue, we use the hybrid data-driven and physics-based approach that models the reservoir inflow based on routinely available rate, pressure and PVT measurements using the proposed transient well performance (TWP) workflow explained below.

2.6. Operating issue detection:

Having the capacity to model the BHP and productivity index, as well as being able to model the expected performance of gas lift and ESPs within the produced fluids and reservoir pressures, allows to approximate a diagnosis of the causes for deviation of expected well performance and forecasted volumes. An additional issue comes from the computation of the critical gas lift rate, or liquid rate required to avoid liquid loading in the well. In total, the tool allows to define 7 basic “production issues”: PI decline, high GOR (from a disruption on the GOR trend and forecasted GOR), liquid loading, up thrusting, down thrusting, and downtime. When compared to the modeled behavior, the deviations observed in the data permit to calculate the required new set points when the issues pertain to the artificial lift system in place, or to recommend an action in the reservoir (acid job) to recover the productivity index.

3. THE SANKEY DIAGRAM: HIGH-GRADED OPTIMIZATION OPPORTUNITIES

To improve time efficiency when monitoring a large well population, the Sankey diagram visualizes the decision tree and its impact across wells with setpoint optimization opportunities. Figure 10 shows a field example, where wells are grouped by artificial lift type, whether a setpoint change is feasible, and the expected revenue impact. The diagram was used in weekly meetings to prioritize wells for action and to track follow-up after setpoint changes were implemented.

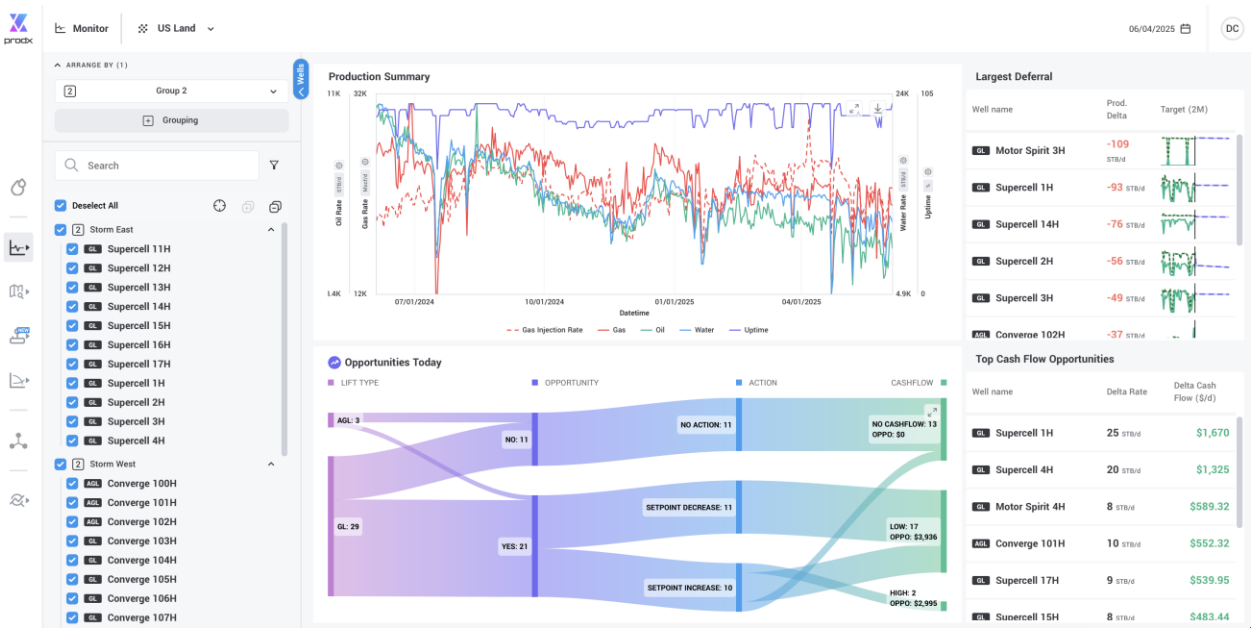

Figure 10 – Sanky diagram for production optimization of different wells within a route based on potential revenue increase and current production deferral.

4. PRODUCTION OPTIMIZATION RESULTS FROM DAILY WELL SURVEILLANCE

4.1. Case Study: Gas Lift Optimization

A total of 49 setpoint changes (31 gas-lift increases and 18 gas-lift decreases) were implemented over three months, optimizing 42 wells across the field. Figure 11 shows the normalized impact of gas lift change on oil rate, aggregated by setpoint type. Deltas were calculated by comparing predicted oil rate (assuming no setpoint change) vs. actual oil rate. On average, a ~29% increase in gas-lift injection delivered a ~4% oil-rate uplift, whereas oil rate remained essentially flat where gas lift was decreased, resulting in a 16% improvement in gas-lift utilization.

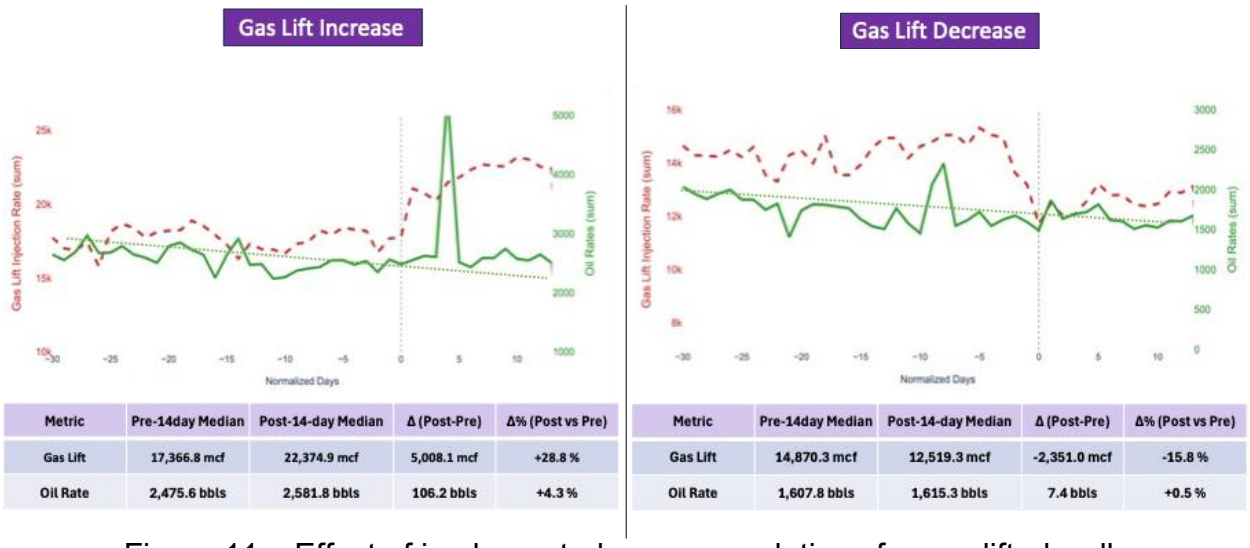

Metric	Pre-14day Median	Post-14-day Median	Δ (Post-Pre)	Δ% (Post vs Pre)
Gas Lift	17,366.8 mcf	22,374.9 mcf	5,008.1 mcf	+28.8 %
Oil Rate	2,475.6 bbls	2,581.8 bbls	106.2 bbls	+4.3 %

Metric	Pre-14day Median	Post-14-day Median	Δ (Post-Pre)	Δ% (Post vs Pre)
Gas Lift	14,870.3 mcf	12,519.3 mcf	-2,351.0 mcf	-15.8 %
Oil Rate	1,607.8 bbls	1,615.3 bbls	7.4 bbls	+0.5 %

Figure 11 – Effect of implemented recommendations for gas lifted wells

4.2. Gas Lift Network optimization

Optimization of centralized gas lift compression networks was made using the network module available in the platform. This model computes the set point for each well to achieve the optimum liquid flow rate while bounded by the maximum GLIR that the shared compressor could provide. In this sense, the available GLIR for the network is assigned on a per-well basis prioritizing those wells with the largest gain in liquid flow rate per scf of gas supplied for lift.

Optimization of shared compression was done for 11 centralized gas lift networks allowing the determination of used capacity of installed for compressors, as well as the need for additional supply. As shown on Figure 12, the optimized point for a full network is bounded for each well by the

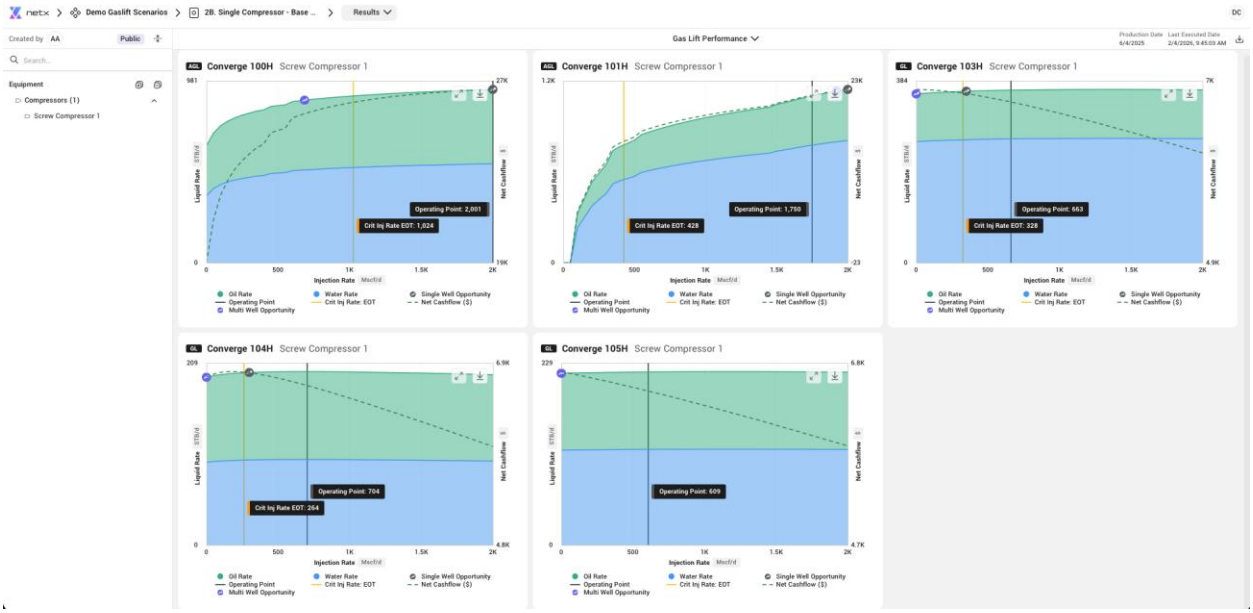

Figure 12 – Centralized gas lift network optimization recommendation

4.3. Case Study: ESP Optimization

On wells with ESPs,14 setpoint changes across 8 wells were implemented as shown in Figure 13. Increasing frequency by ~7 Hz on average increased oil rate by 7% across 5 wells. On 3 wells where frequency was decreased a 3.5% increase in oil rate was observed over a 14-day period.

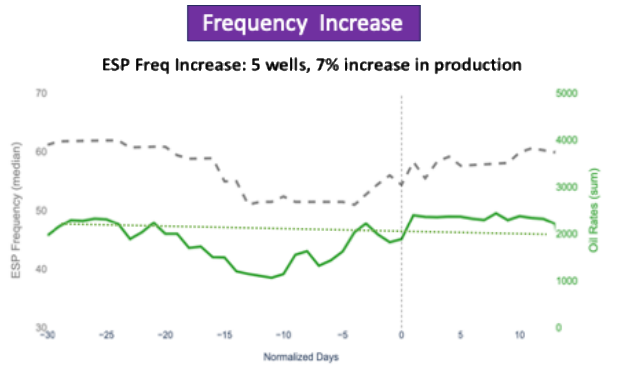

Metric	Pre-14day Median	Post-14-day Median	Δ (Post-Pre)	Δ% (Post vs Pre)
ESP Frequency	51.5 Hz	58.3 Hz	6.8 Hz	+13.2 %
Oil Rate	2,196.9 bbls	2,353.1 bbls	156.2 bbls	+7.1 %

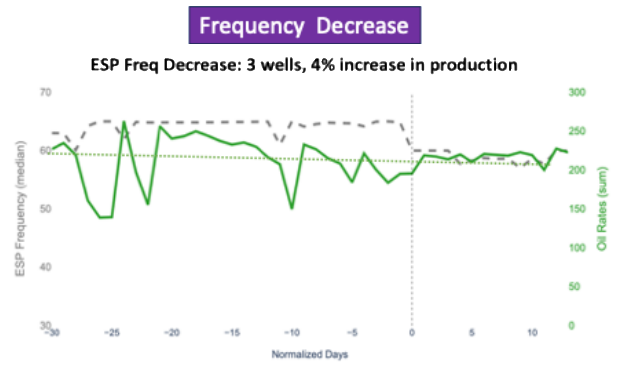

Metric	Pre-14day Median	Post-14-day Median	Δ (Post-Pre)	Δ% (Post vs Pre)
ESP Frequency	64.8 Hz	58.6 Hz	-6.2 Hz	-9.5 %
Oil Rate	211.8 bbls	219.2 bbls	7.4 bbls	+3.5 %

Figure 13 – Impact on oil production of implemented ESP setpoint recommendations.

4.4. Acid job performance evaluation

A total of 256 acid jobs performed over a period of two years were evaluated upon their impact on the productivity index (PI) of the well. On a per-well basis the impact of an acid job can be observed on an increase of production, but the typical unpacking behavior after restarting the well, makes it difficult to quantify the production increase as well as the effect that the acid job had on the flowing capacity of the tubing and the matrix. When considering the PI, a better perspective is obtained to evaluate the total effect of the acid job on the system, as shown in Figure 14. Using this data from all the acidized jobs allows to understand an expected average outcome of an acid job in terms of the PI.

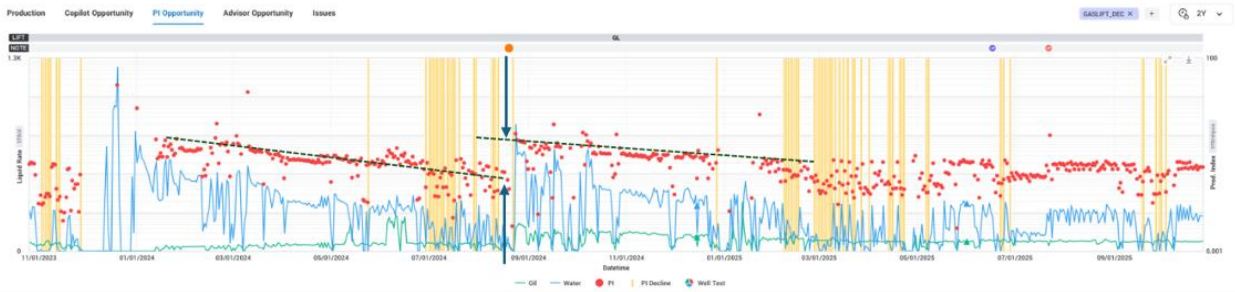

Figure 14 – Production and productivity index of a well impacted by an acid job

In this work, a statistical analysis was done to forecast an average acid job impact as a function of the PI at the moment of implementing the intervention. The acid job impact was defined as the percentual change on the productivity index before and after the job, as shown on equation 3.

$$PI_{impact} = \frac{PI_{after}}{PI_{before}} - 1 \qquad \text{Eq 3}$$

Among the analyzed variables it was included the type of rig used for the job, the geologic formation of the reservoir as well as the production conditions and issues existing in the well for all the acid jobs performed.

As shown in Figure 15, an exponential regression obtained from the PI impact vs the PI at time of implementation, suggests an average PI impact of 59%, and that no more than 3 times the original PI could be achieved after an acid job. From a statistical point of view, the rate of change of the PI impact vs. the PI at the moment of implementing the acid job, indicated that the “ideal PI” for implementation was when nearing 0,18 bpd/psi of liquid (about 0.02 bpd/psi of oil). At this “ideal PI”, an inflection was observed for the PI impact suggesting that larger PI values would not yield such a growth on the PI, and below, the well was causing an undesired deferment.

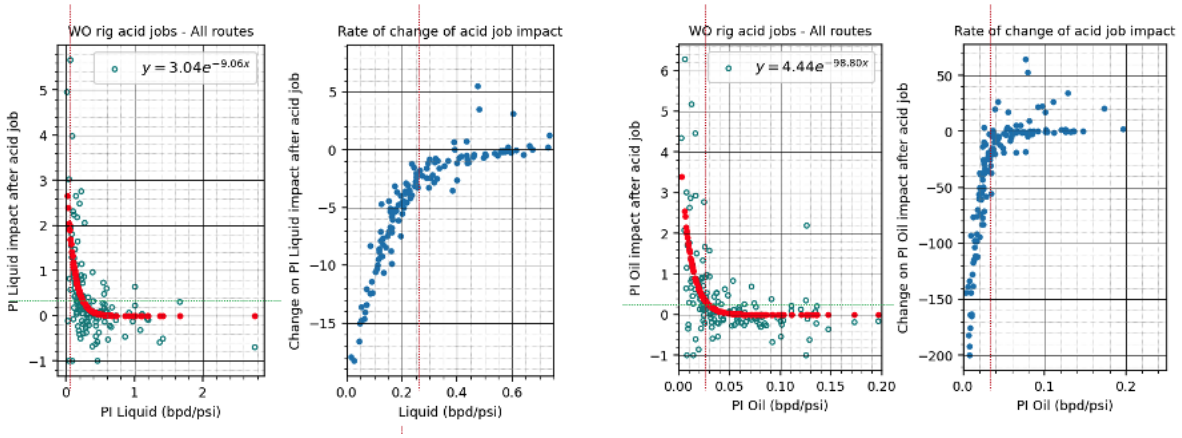

Figure 15 – Acid job impact on the PI of the well when using workover rigs.

When performing this analysis in terms of the oil production, slightly larger values were obtained for the PI impact (62%) as shown in Figure 16, suggesting relatively better oil permeability after the job. It must also be considered that acid content in the flowback after the job or maintenance to the oil flowmeters could also yield on larger oil flowrate readings.

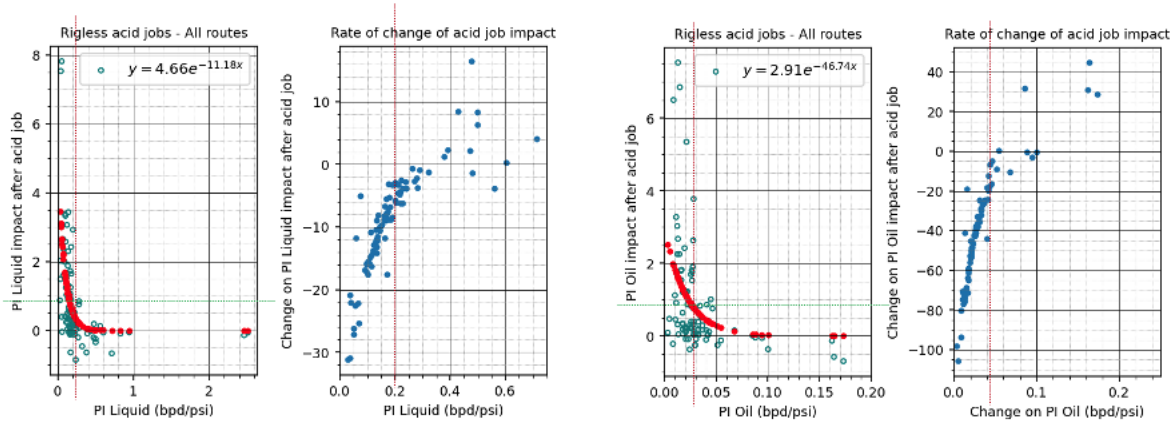

Figure 16 - Acid job impact on the PI of the well when performing rigless jobs.

No statistical difference was observed between the results from rigless jobs and those with workover rigs (Figure 16) in terms of the ideal PI for implementation (about 0.18 PI liquid and 0.02 PI oil for both) and the expected PI impact average (60% for both)

The impact on the productivity for each acid job was tabulated and compared, considering the detected production issues in the well before the acid job. As shown on Figure 17, 12% of all the jobs performed were done on wells with PI decline issues. Among these wells, the average PI impact was of 75%, which is statistically larger than the 60% value obtained for the entire population. The ideal PI was still within 0.02 bpd/psi, as shown on Figure 18.

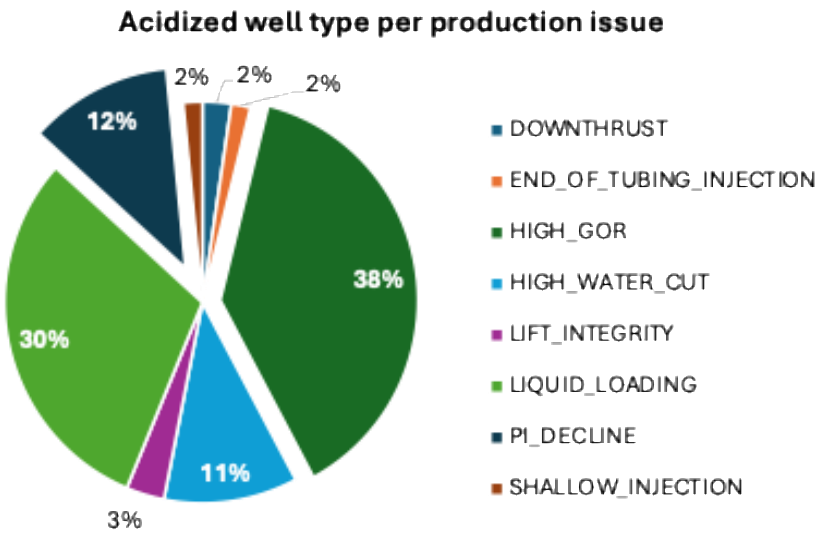

Figure 17 – Share of wells according to the production issues among acidized wells.

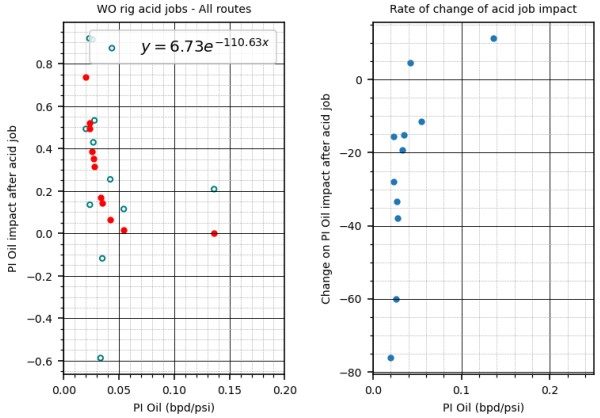

Figure 18 - Acid job impact on the PI of the well when using a workover on wells with PI decline issues.

5. ARTIFICIAL LIFT SYSTEM TRANSITION – SCENARIO MODELING

As reservoir pressure declines over time, artificial lift systems can become inefficient at producing liquids to surface. Previously installed ESPs can become oversized relative to decreasing liquid rates and increasing GLR. ESP tornado plots help identify when an ESP is operating in this regime; however, evaluating a future, smaller design is not possible unless nodal analysis is performed under current and forecasted reservoir conditions. Leveraging TWP analysis, it is possible to forecast well production rates based on PI, compute the BHP at which operation is no longer stable, and evaluate transition options (e.g., a smaller ESP or gas lift).

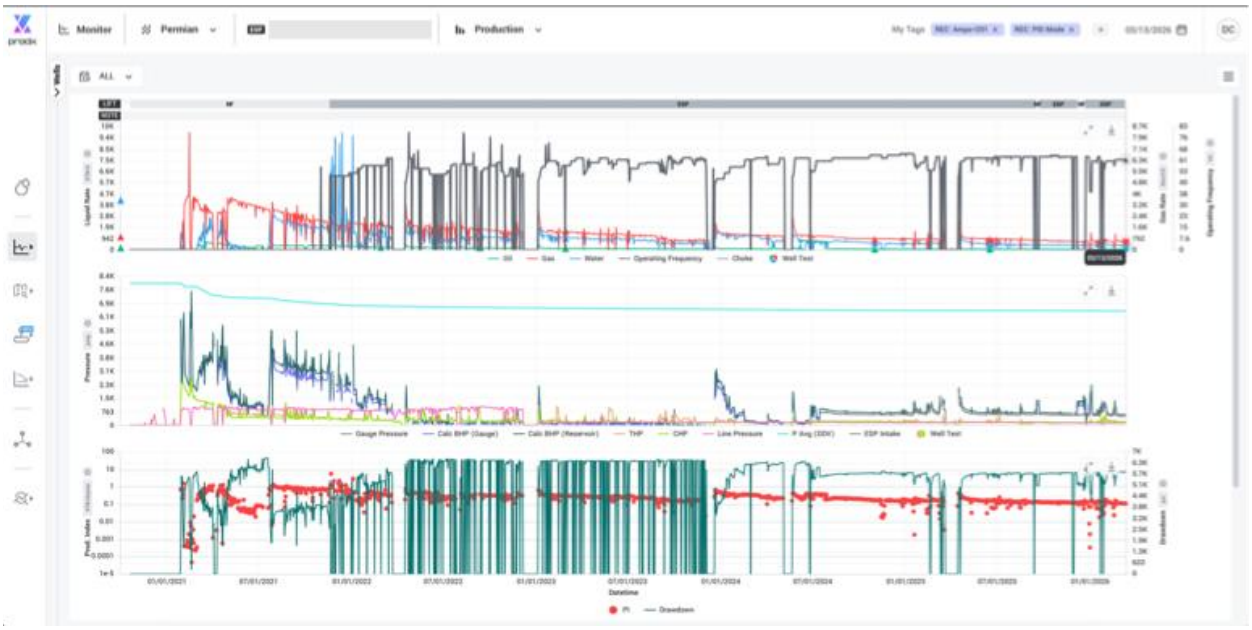

Figure 19 – Production history of an example well.

Figure 19 shows the liquid rate data of a well in the Wolfcamp B in production since 2012, currently operating with a FlexER 17.5, with a BEP at 1750 bpd of liquid, delivering 573 mscfd of gas and nearly 400 bpd, which is less than 25% of the BEP liquid rate of the pump. As shown on Figure 20, the operation of the pump has become unstable, with an average electric current of 220 amps fluctuating +/- 27%, reaching a peak of 256 amps, close to the 263 amp limit, as the pump operates in frequency mode set at 61 Hz. The platform suggests that the ESP shall be put in PID mode, with a setpoint of 200 amps, as indicated on the upper right corner of the figure.

Figure 20 – High frequency SCADA data of the example well.

The tornado pump shown in Figure 21 indicates that the instability of the pump has increased in the past 6 months, and the recommended set point computed by the software to extend the operating life of the equipment is 35 Hz (to allow an easier management of the GVF in the stages), in sacrifice of liquid production.

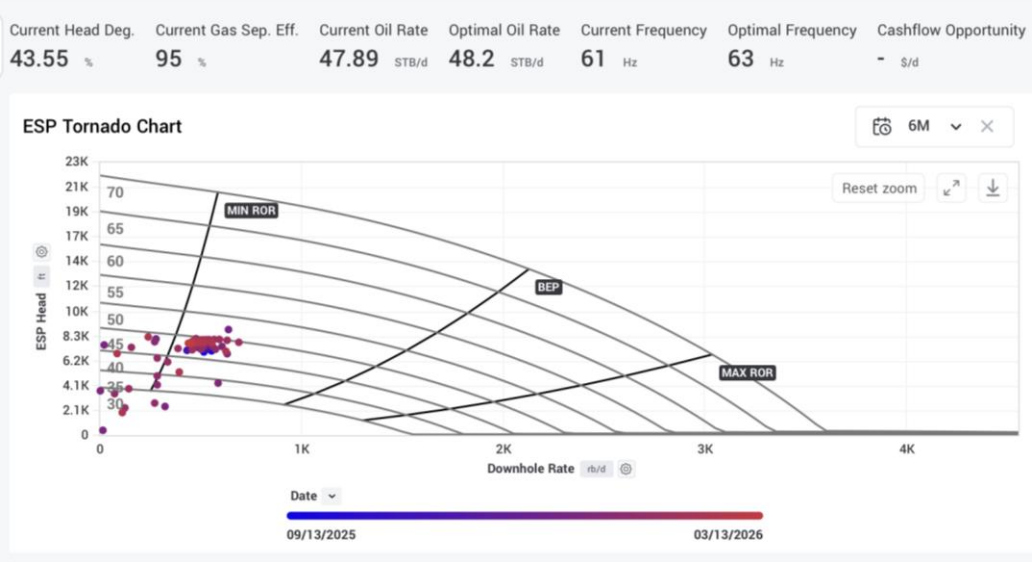

Figure 21 – Tornado plot of the example well

The maximum recommended frequency computed in the software is 63 Hz as shown in Figure 22 (indicated by the red circle on the surface performance plot) approaching to the surge point which is expected to be 64 Hz Indicated by a red line on the downhole performance plot.

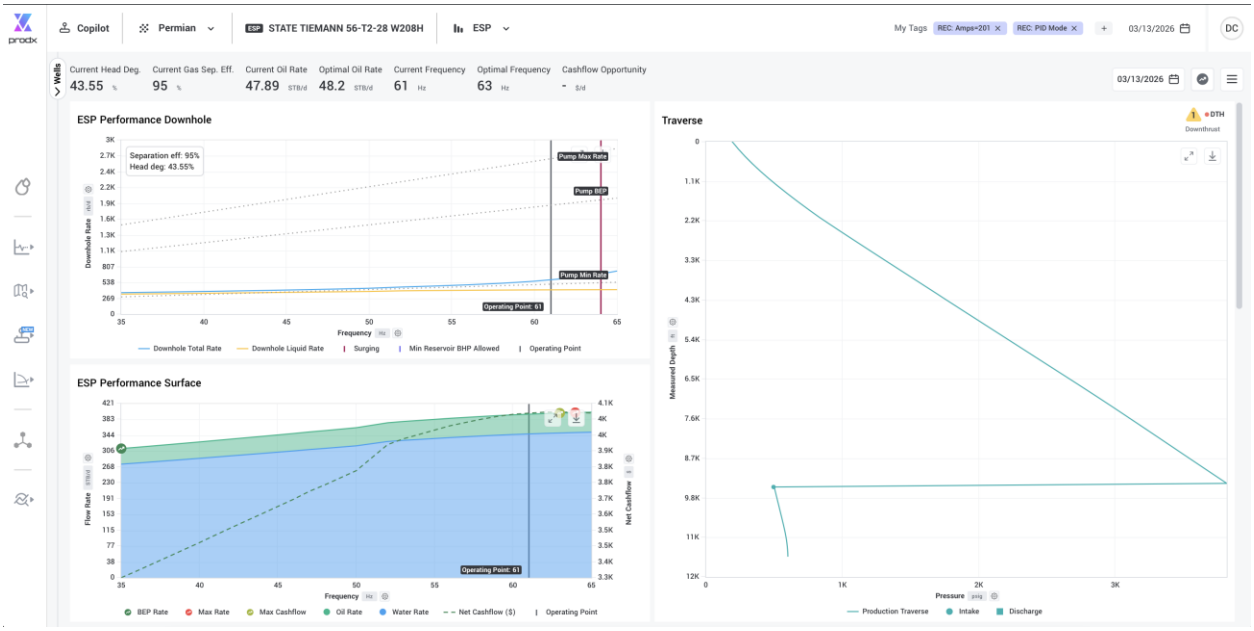

Figure 22 – Surface and downhole plots of the example well

Considering the low liquid rates relative to the BEP, the high and fluctuating electric current and deteriorating performance in time, it was evaluated a smaller ESP scenario, along with gas lift through tubing and through annular flow. The smaller ESP is composed of sections of E1000 stages and gas handlers, operating at 58 Hz with an estimated head degradation of 17% and gas separation efficiency of 80%. The gas lift scenarios consider a GLIR of 900 mscfd, with an injection pressure of 1200 psi.

As seen in Figure 23, the small-ESP option offers the largest rate among the considered options, delivering about 415 bpd, which is ~2 bpd less liquid than the current ESP (and ~1 bpd lower oil rate, based on a water cut of 89%).

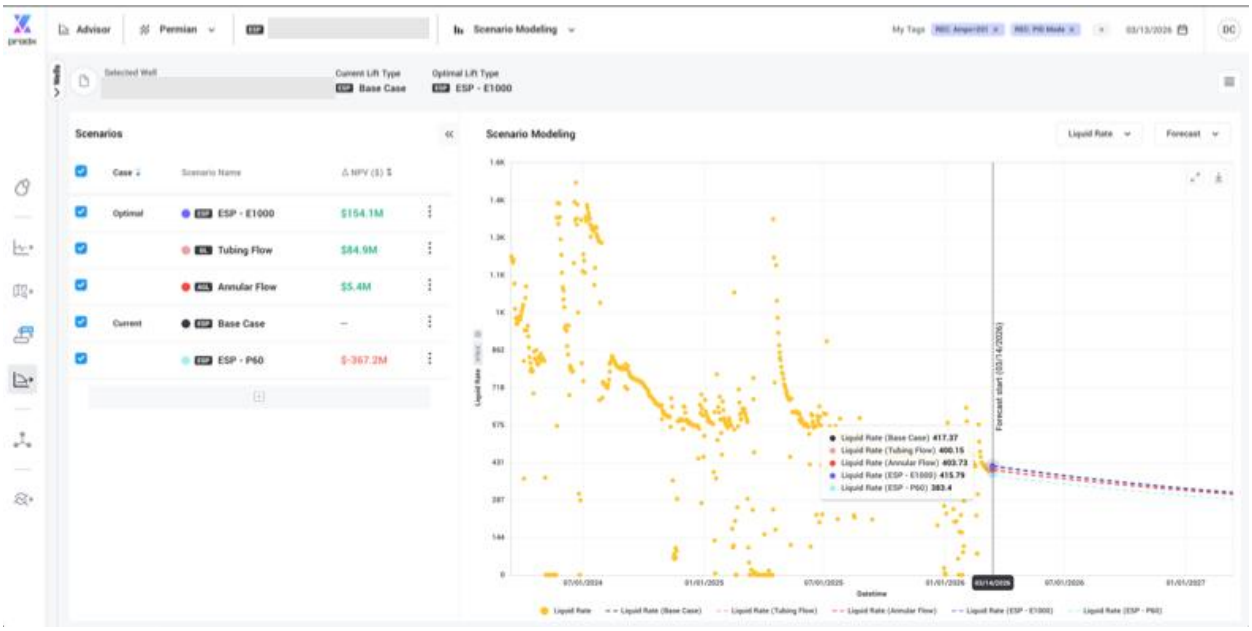

Figure 23 – Scenario modeling of an example well

The additional revenue from the smaller-ESP option compared to the current ESP (+\$154 thousand over a two-year period) is offset by an expected replacement of the ESP currently in the wellbore (indicated by an early drop in the baseline revenue, as shown in Figure 24). This estimate comes from a statistical analysis of the operating life of all ESPs across the production history of wells participating in the pilot.

Figure 24 – Forecasted revenue for different artificial lift scenarios for the example wells.

6. ADOPTION CHALLENGES

The adoption of the digital optimization platform during the pilot phase revealed several practical barriers, which are further evidenced by the rejection patterns summarized in Figure 25. The distribution of rejected recommendations provides a direct, field-level validation of the underlying adoption challenges, highlighting that successful deployment is not solely a function of model accuracy, but rather of data readiness, workflow integration, and organizational alignment.

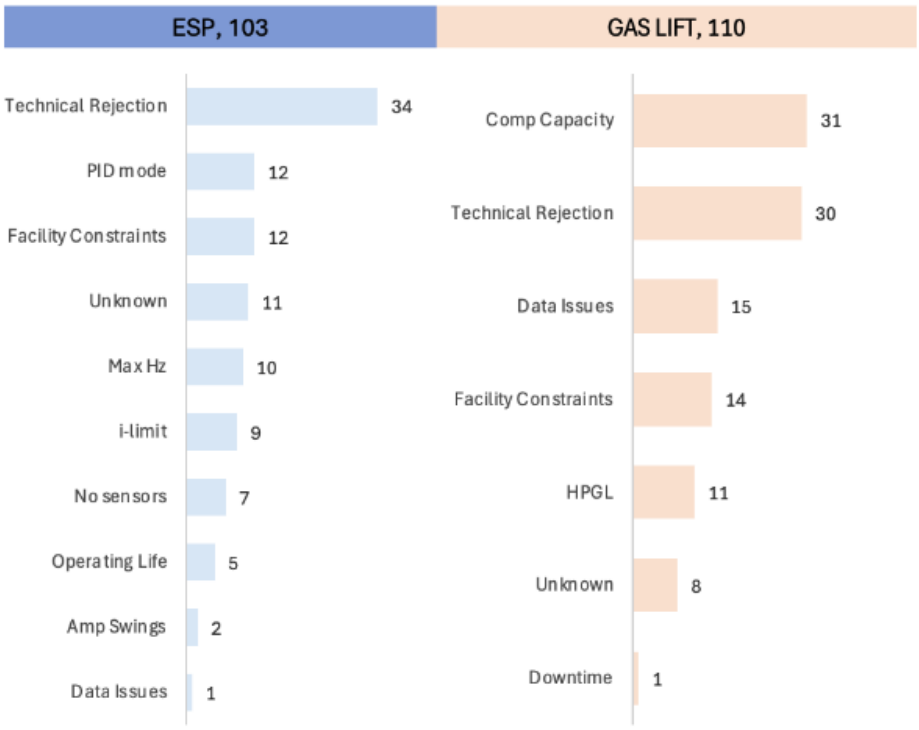

Figure 25 – Primary Drivers of Recommendation Rejection Highlighting Key Adoption Barriers

6.1 Technical Rejection and Trust Gap

As shown in Figure 25, *technical rejection* represents the largest category of rejected recommendations for both ESP (34 cases) and Gas Lift wells (30 cases). This trend reflects a combination of interrelated adoption challenges.

First, there exists an inherent trust gap during early deployment stages, where engineers are reluctant to act on recommendations that do not align with their experience or established heuristics. This is particularly evident when the system's outputs lack transparency or are not easily reconcilable with known well behavior.

Second, cross-functional coordination challenges contribute to technical rejection. Effective implementation requires alignment between petroleum engineers, field

operators, and data/IT teams. In the absence of clear ownership and feedback loops, recommendations may not be executed or validated, leading to rejection.

Third, misalignment with existing workflows and KPIs further exacerbates this issue. Recommendations that conflict with current operating practices or do not clearly map to established performance metrics are less likely to be adopted.

Finally, platform limitations in capturing real-world complexity—particularly in early-stage deployments—also contribute to technical rejection. For example, ESP-related recommendations based on daily average data failed to capture short-term instabilities, reducing their perceived reliability until higher-frequency (SCADA-driven) logic was incorporated.

Collectively, these factors indicate that "technical rejection" is not solely a model deficiency, but rather a composite signal of trust, integration, and model maturity gaps.

6.2 Data Availability and Quality Constraints

Data-related challenges remain a foundational barrier to adoption. As highlighted in Figure 25, *data issues* account for a notable portion of rejected recommendations, particularly in Gas Lift operations (15 cases).

The effectiveness of the platform relies on the availability of both static data (e.g., well configuration, tubing/casing details) and dynamic data (e.g., production rates, pressures, and setpoints). However, in many cases, data is fragmented across multiple systems, inconsistently formatted, or incomplete due to historical gaps and asset transfers. These limitations directly impact the reliability of model outputs, leading to reduced confidence and increased rejection rates. Consequently, an initial onboarding phase focused on wells with the most complete datasets is critical for demonstrating value.

6.3 Lack of Continuous Data Infrastructure

A related challenge is the absence of automated, continuous data pipelines. The platform requires consistent ingestion of both daily production data and high-frequency SCADA data to generate accurate recommendations.

In many cases, such infrastructure is not readily available, and data delivery relies on manual processes. This not only delays analysis but also introduces inconsistencies, further contributing to rejection of recommendations. The implementation of API-driven data pipelines, supported by IT and data management teams, is therefore essential to enable scalable and sustainable adoption.

6.4 Surface and Network Constraints

Figure 25 also highlights the impact of surface and network limitations, including compressor capacity (31 cases), facility constraints (14–12 cases), and HPGL limitations (11 cases).

These constraints indicate that recommendations generated at the well level may not always be feasible within the broader system context. The absence of integrated network modeling leads to scenarios where technically valid recommendations are operationally infeasible, resulting in rejection. This underscores the importance of incorporating facility-level and network-level constraints into the optimization framework to improve recommendation viability.

6.5 Operational and Control System Alignment (ESP-Specific)

For ESP wells, additional rejection categories such as *PID mode (12)*, *Max Hz (10)*, *i-limit (9)*, and *sensor limitations (7)* reflect challenges in aligning the platform with existing control systems and operational practices.

These findings indicate that early implementations, which relied primarily on daily average data, were insufficient to capture high-frequency operational dynamics such as motor current fluctuations and instability events. The subsequent introduction of SCADA-driven logic (e.g., PID-based control recommendations) significantly improved acceptance rates. This highlights the need for platform adaptability to align with real-time operational behavior and control strategies.

6.6 Feedback Loop and Decision Transparency

A non-negligible portion of rejections is categorized as *unknown* (ESP: 11, Gas Lift: 8), as shown in Figure 25. This suggests a lack of structured feedback mechanisms to capture the rationale behind decision-making.

The absence of clear feedback loops limits the ability to refine models, improve recommendations, and build user trust over time. Establishing systematic processes for tracking, categorizing, and analyzing rejected recommendations is therefore critical for continuous improvement.

6.7 Summary

The analysis of rejection patterns in Figure 25 demonstrates that adoption challenges are multifaceted and tightly coupled with operational realities. While model accuracy is necessary, it is not sufficient to drive adoption.

Successful implementation requires:

- High-quality, accessible data
- Continuous and automated data pipelines

- Alignment with existing workflows and KPIs
- Integration of network and facility constraints
- Adaptability to real-time operational dynamics
- Strong cross-functional collaboration and feedback loops

Ultimately, adoption is driven by trust, usability, and integration into existing decision-making processes, as much as by the technical robustness of the underlying models.

7. REFERENCES

- Besler, M.R., Steele, J.W., Egan, T., and Wagner, J. 2007. Improving Well Productivity and Profitability in the Bakken: A Summary of Our Experiences Drilling, Stimulating, and Operating Horizontal Wells. Paper SPE 110679 presented at the SPE Annual Technical Conference and Exhibition, Anaheim, CA, 11-14 November.
- Molinari, D., and Sankaran, S. 2021. "A Reduced Physics Modeling Approach to Understand Multiphase Well Production Performance for Unconventional Reservoirs." URTEC-2021-5023-MS, SPE/AAPG/SEG Unconventional Resources Technology Conference, Houston, Texas, USA. doi: https://doi.org/10.15530/urtec-2021-5023
- Molinari, D., Sankaran, S., Symmons, D., and Perrotte, M. 2019. "A Hybrid Data and Physics Modeling Approach Towards Unconventional Well Performance Analysis." SPE-196122-MS, SPE Annual Technical Conference and Exhibition, Calgary, Alberta, Canada: 1-27. doi: https://doi.org/10.2118/196122-MS
- Molinari, D., Sankaran, S., Symmons, D., Perrotte, M., Wolfram, E., Krane, I., Han, J., and Bansal, N. 2019. "Implementing an Integrated Production Surveillance and Optimization System in an Unconventional Field." URTEC-2019-41-MS, SPE/AAPG/SEG Unconventional Resources Technology Conference, Denver, Colorado, USA: 1-19. doi: https://doi.org/10.15530/urtec-2019-41
- Parekh, Bimal, Hardik Kumar Zalavadia, Haiwen Zhu, Amir Fallah, Matthew Wortmann, Matthew Dupree, and Chad Harbaugh. "Case study on continuous unconventional production surveillance and optimization using automated hybrid modeling approach." In *SPE/AAPG/SEG Unconventional Resources Technology Conference*, p. D031S050R003. URTEC, 2025.
- Pradhan, Y. 2020. "Observed Gas-Oil Ratio Trends in Liquids Rich Shale Reservoirs." URTEC-2020-3229-MS, SPE/AAPG/SEG Unconventional Resources Technology Conference, Virtual: 1-15. doi: https://doi.org/10.15530/urtec-2020-3229
- Price, L.C. 1986. Organic Metamorphism in the Lower Mississippian upper Devonian Bakken Shale. Journal of Petroleum Geology. 9:313-342
- Rahman, M., Gioria, G., Sankaran, S., and Molinari, D. 2019. "Automatic Well Interference Identification and Characterization: A Data-Driven approach to Improve Field Operation." SPE-195813-MS, SPE Annual Technical Conference

and Exhibition, Calgary, Alberta, Canada: 1-21. doi: https://doi.org/10.2118/195813-MS

- Sankaran, S., Lugo, J., Awasthi, A. and Mijares, G. "The Promise and Challenges of Digital Oilfield Solutions—Lessons Learned from Global Implementations and Future Directions." Paper presented at the SPE Digital Energy Conference and Exhibition, Houston, Texas, USA, April 2009. doi: https://doi.org/10.2118/122855-MS
- Simpson, G.A., and Fishman, N.S., 2015, Unconventional tight oil reservoirs—a call for new standardized core analysis workflows and research: SCA2015-Paper 022, International Symposium of the Society of Core Analysts, 12 p.
- Wortmann, M., Zhu, H., Zalavadia, H., James, C., & Harbaugh, C. (2025, June). Case study on real-time pump health check for optimizing ESP performance and extending lifespan in unconventional wells. In *SPE/AAPG/SEG Unconventional Resources Technology Conference* (p. D021S038R002). URTEC.
- Xue X., Yang C., Park J., Sharma V. K., Datta-Gupta, A., and King, M.J. 2019. "Reservoir and Fracture-Flow Characterization Using Novel Diagnostic Plots." SPE J. 24: 1248–1269. doi: https://doi.org/10.2118/194017-PA